Modelling low-mass, main sequence stars: radius discrepancy and magnetic activity

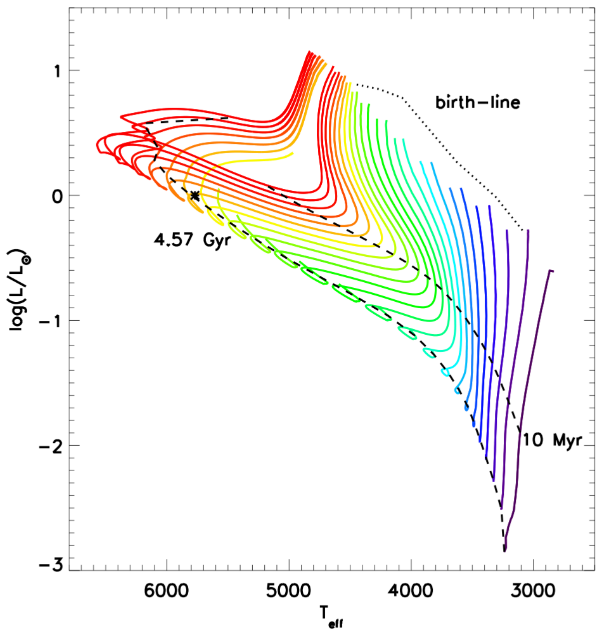

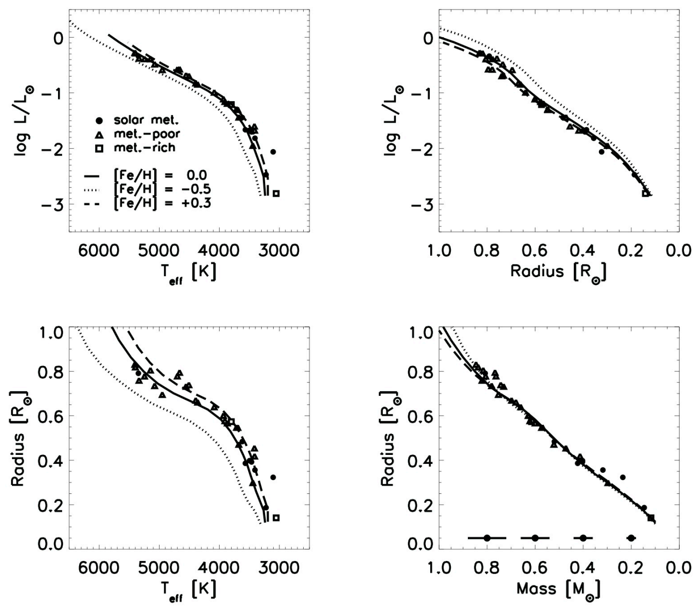

Federico Spada

Leibniz Institut für Astrophysik (AIP), Potsdam, Germany

Outline

- Motivation
- Modelling low mass stars
- The “radius discrepancy”
- Stellar models with magnetic fields
- Summary

Motivation

- Stars with subsurface CZ: solar-like dynamo, magnetic activity, wind braking and rotational evolution…
- Promising candidates as exoplanets hosts
- Knowledge of fundamental parameters of these stars is very valuable
- “Radius discrepancy”

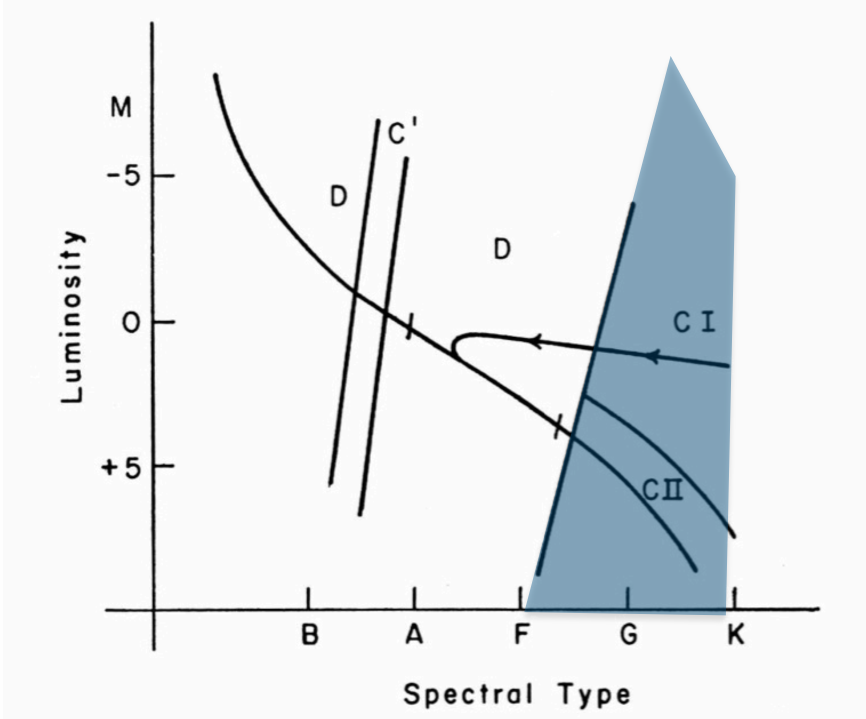

Schatzman (1960)

AIP

YREC: the Yale Rotational stellar Evolution Code

Standard input physics

- OPAL opacities
- Standard mixing length theory of convection
- **OPAL 2005 EOS**
- Element diffusion
- **Grey atmosphere T(τ) relation (e.g. Eddington)**

Structural effect of rotation

$$\frac{d\log P_\psi}{d\log M_\psi} = -f_P \frac{GM_\psi^2}{4\pi r_\psi^4 P_\psi} \quad (1)$$

$$\frac{d\log T_\psi}{d\log M_\psi} = \nabla \frac{d\log P_\psi}{d\log M_\psi} \quad \text{where } \nabla = \frac{d\ln T}{d\ln P} = \min\left\{\nabla_{conv}, \frac{f_T}{f_P}\nabla_{rad}\right\} \quad (2)$$

$$\frac{d\log r_\psi}{d\log M_\psi} = \frac{M_\psi}{4\pi r_\psi^3 \rho}, \text{ and} \quad (3)$$

$$\frac{dL_\psi}{d\log M_\psi} = \frac{M_\psi}{L_o}\ln 10\left\{\varepsilon - T_\psi \frac{dS}{dt}\right\}, \quad (4)$$

Rotational evolution

$$\frac{dJ}{dt} = -K\omega^3\left(\frac{R}{R_\odot}\right)^{0.5}\left(\frac{M}{M_\odot}\right)^{-0.5}, \quad \omega \le \omega_{crit},$$

$$\frac{dJ}{dt} = -K\omega_{crit}^2\,\omega\left(\frac{R}{R_\odot}\right)^{0.5}\left(\frac{M}{M_\odot}\right)^{-0.5}, \quad \omega > \omega_{crit}.$$

Modelling low mass stars ($M \leq 0.6\ M_\odot$): additional challenges

- **Surface boundary conditions**:
  - Formation of H_2 leads to atmospheric convection
  - Molecular contribution to opacity
- **Equation of State:**
  - Low central temperature, high density: non-ideal effects

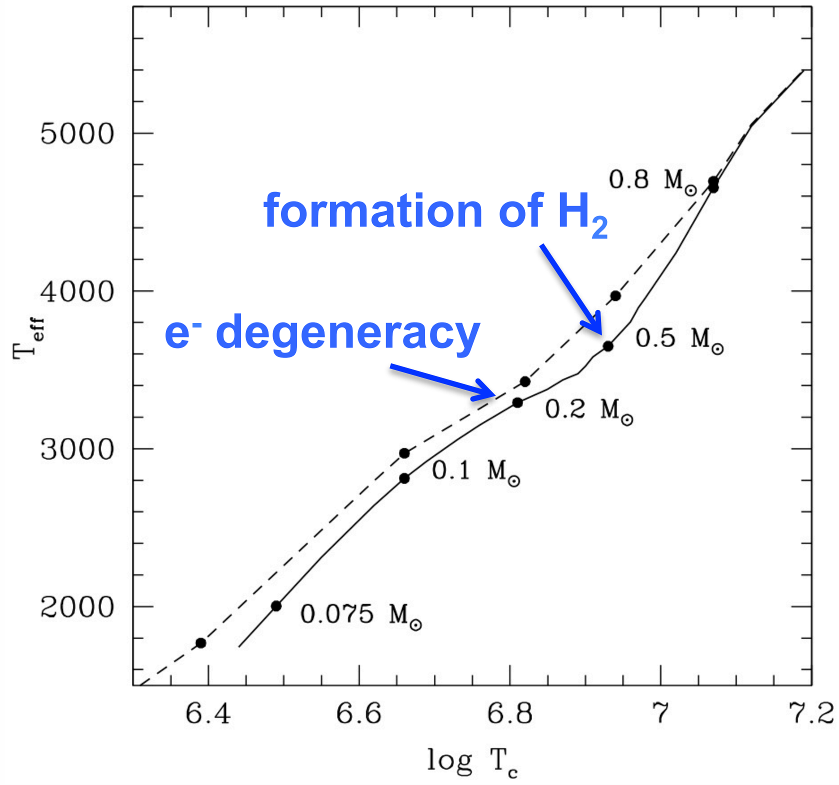

After Baraffe et al. (1998)

Improved YREC configuration

Surface BC

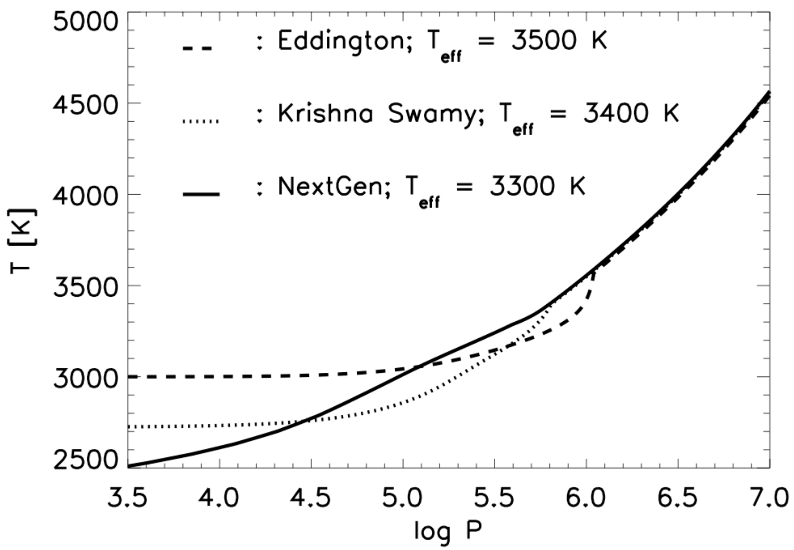

Non-grey atmospheres: **PHOENIX “BT-Settl” models**

EOS

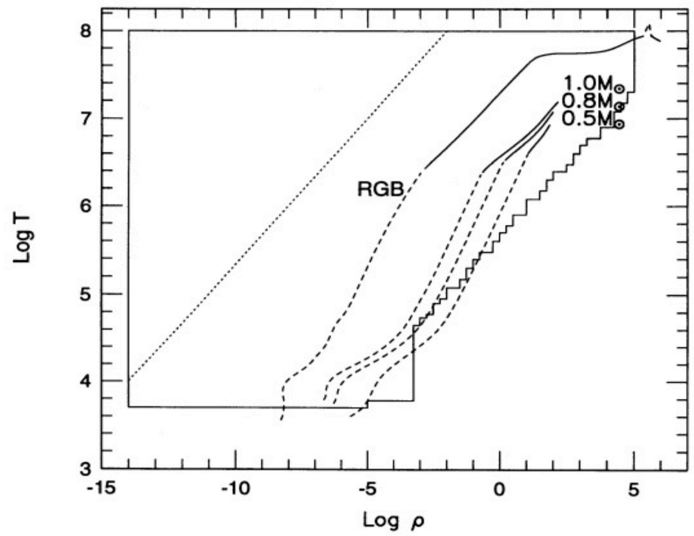

SCVH EOS in the low T/high ρ regime (*Saumon et al. 1995*)

The grid

- $M = 0.10 \div 1.25\ M_\odot$
- $[Fe/H] = +0.3, 0.0, -0.5, -1.0, -1.5$
- $Y = Y_p + (\Delta Y/\Delta Z)\ Z$
- No rotation
- Standard solar model calibration:
  - $\alpha = 1.875$
  - $\Delta Y/\Delta Z = 1.48$

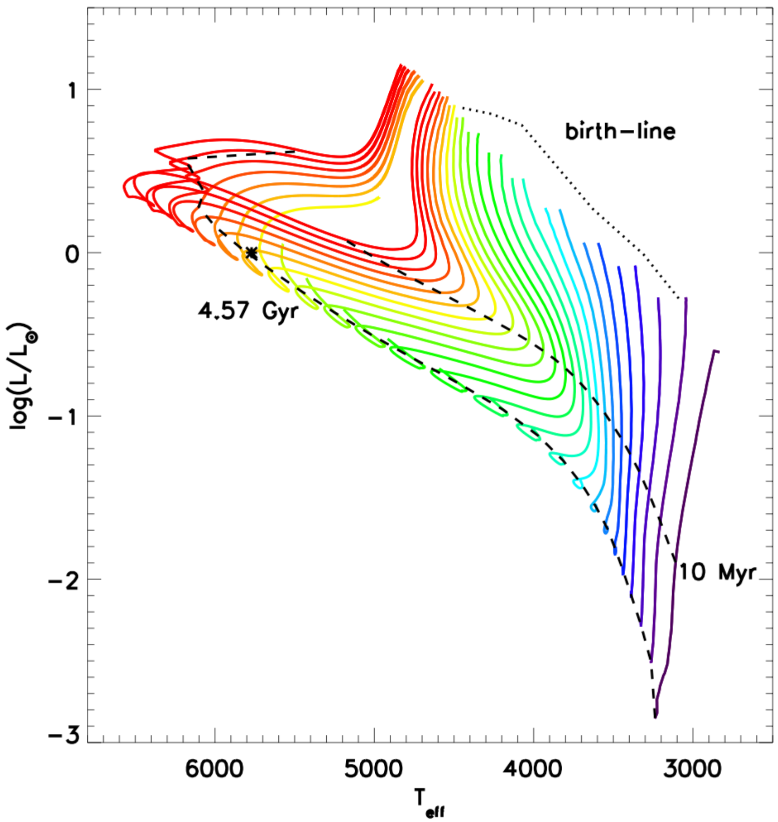

F. Spada, P. Demarque, Y. -C. Kim and A. Sills (in subm.)

AIP

Double-lined eclipsing binaries

- Most recent compilation: *Feiden & Chaboyer (2012)*
- M, R known at least to better than 5%
- Some information on age, metallicity
- T_{eff} unknown or poorly constrained

Star Name	P_{orb} (day)	Mass ($M_\odot$)	Radius ($R_\odot$)	P_{rot} (day)	Source
UV Psc A	0.86	0.9829 ± 0.0077	1.110 ± 0.023	...	1
UV Psc B		0.76440 ± 0.00450	0.8350 ± 0.0180	0.80	
IM Vir A	1.309	0.981 ± 0.012	1.061 ± 0.016	...	2
IM Vir B		0.6644 ± 0.0048	0.6810 ± 0.013	1.31	
KID 6131659 A	17.528	0.924 ± 0.008	0.8807 ± 0.0017	...	3
KID 6131659 B		0.683 ± 0.005	0.6392 ± 0.0013	...	
RX J0239.1-1028 A	2.072	0.7300 ± 0.0090	0.7410 ± 0.0040	...	4
RX J0239.1-1028 B		0.6930 ± 0.0060	0.7030 ± 0.0020	...	
Kepler-16 A	41.08	0.6897 ± 0.0034	0.6489 ± 0.0013	...	5
Kepler-16 B		0.20255 ± 0.0007	0.22623 ± 0.0005	...	
GU Boo A	0.49	0.61010 ± 0.00640	0.6270 ± 0.0160	0.49	6
GU Boo B		0.59950 ± 0.00640	0.6240 ± 0.0160	0.54	
YY Gem A	0.81	0.59920 ± 0.00470	0.6194 ± 0.0057	0.87	7
YY Gem B		0.59920 ± 0.00470	0.6194 ± 0.0057	0.82	
MG1-506664 A	1.55	0.584 ± 0.002	0.560 ± 0.005	...	8
MG1-506664 B		0.544 ± 0.002	0.513 ± 0.009	...	
MG1-116309 A	0.827	0.567 ± 0.002	0.552 ± 0.004	...	8
MG1-116309 B		0.532 ± 0.002	0.532 ± 0.004	...	
MG1-1819499 A	0.630	0.557 ± 0.001	0.569 ± 0.002	...	8
MG1-1819499 B		0.535 ± 0.001	0.500 ± 0.003	...	
NSVS 01031772 A	0.368	0.5428 ± 0.0027	0.5260 ± 0.0028	...	9
NSVS 01031772 B		0.4982 ± 0.0025	0.5088 ± 0.0030	...	
MG1-78457 A	1.586	0.527 ± 0.002	0.505 ± 0.008	...	8
MG1-78457 B		0.491 ± 0.001	0.471 ± 0.009	...	
MG1-646680 A	1.64	0.499 ± 0.002	0.457 ± 0.010	...	8
MG1-646680 B		0.443 ± 0.002	0.427 ± 0.008	...	
MG1-2056316 A	1.72	0.469 ± 0.002	0.441 ± 0.004	...	8
MG1-2056316 B		0.382 ± 0.001	0.374 ± 0.004	...	
CU Cnc A	2.77	0.43490 ± 0.00120	0.4323 ± 0.0055	...	10
CU Cnc B		0.39922 ± 0.00089	0.3916 ± 0.0094	...	
LSPM J1112+7626 A	41.03	0.3946 ± 0.0023	0.3860 ± 0.0052	...	11
LSPM J1112+7626 B		0.2745 ± 0.0012	0.2978 ± 0.0046	...	
KOI-126 B	1.77	0.2413 ± 0.0030	0.2543 ± 0.0014	...	12
KOI-126 C		0.2127 ± 0.0026	0.2318 ± 0.0013	...	
CM Dra A	1.27	0.23102 ± 0.00089	0.2534 ± 0.0019	...	13
CM Dra B		0.21409 ± 0.00083	0.2398 ± 0.0018	...	

References. (1) Popper 1997; (2) Morales et al. 2009b; (3) G. Bass et al. (2012, in preparation); (4) López-Morales & Shaw 2007; (5) Doyle et al. 2011; (6) López-Morales & Ribas 2005; (7) Torres & Ribas 2002; (8) Kraus et al. 2011; (9) López-Morales et al. 2006; (10) Ribas 2003; (11) Irwin et al. 2011; (12) Carter et al. 2011; (13) Morales et al. 2009a.

AIP

Single stars interferometric measurements

- *Boyajian et al. (2012)*
- R, T_{eff}, L known better than a few %
- Literature estimates for Z
- Comparatively **large** (~10%) **error on mass**

Fundamental Parameters

Star Name	Spectral Type	Metallicity [Fe/H]	Metallicity Reference[a]	$R \pm \sigma$ ($R_\odot$)	Radius Reference[b]	$F_{BOL} \pm \sigma$ (10^{-8} erg cm s^{-2})	$L \pm \sigma$ ($L_\odot$)	$T_{EFF} \pm \sigma$ (K)	Mass ($M_\odot$)	L_X/L_{BOL}
GJ 15A†	M1.5 V	−0.36	1	0.3874 ± 0.0023	This work	5.420 ± 0.044	0.02173 ± 0.00021	3563 ± 11	0.423	2.32E−05
GJ 33	K2 V	−0.22	2	0.6954 ± 0.0041	This work	15.060 ± 0.100	0.26073 ± 0.00263	4950 ± 14	0.753	8.59E−07
GJ 105	K3 V	−0.08	2	0.7949 ± 0.0062	This work	16.680 ± 0.103	0.26790 ± 0.00239	4662 ± 17	0.767	1.70E−06
GJ 166A†	K1 Ve	−0.24	2	0.8061 ± 0.0036	This work	52.690 ± 0.394	0.40782 ± 0.00319	5143 ± 14	0.816	1.03E−05
GJ 205	M1.5 V	0.35	3	0.5735 ± 0.0044	This work	6.182 ± 0.032	0.06163 ± 0.00088	3801 ± 9	0.615	1.62E−05
GJ 338A	M0.0 V	−0.18	3	0.5773 ± 0.0131	This work	5.885 ± 0.051	0.06974 ± 0.00213	3907 ± 35	0.622	2.07E−05
GJ 338B	K7.0 V	−0.15	3	0.5673 ± 0.0137	This work	5.455 ± 0.037	0.06465 ± 0.00194	3867 ± 37	0.600	2.23E−05
GJ 380†	K7.0 V	−0.16	2	0.6415 ± 0.0048	This work	13.860 ± 0.093	0.10253 ± 0.00088	4081 ± 15	0.660	6.92E−06
GJ 411†	M2.0 V	−0.41	3	0.3921 ± 0.0037	This work	9.842 ± 0.060	0.01989 ± 0.00014	3465 ± 17	0.403	8.03E−06
GJ 412A	M1.0 V	−0.40	3	0.3982 ± 0.0091	This work	2.908 ± 0.022	0.02129 ± 0.00026	3497 ± 39	0.403	3.11E−05
GJ 526	M1.5 V	−0.30	3	0.4840 ± 0.0084	This work	3.979 ± 0.030	0.03603 ± 0.00051	3618 ± 31	0.520	5.33E−06
GJ 631	K0 V	0.04	2	0.7591 ± 0.0122	This work	14.160 ± 0.090	0.41945 ± 0.00422	5337 ± 41	0.821	8.92E−06
GJ 687	M3.0 V	−0.09	3	0.4183 ± 0.0070	This work	3.332 ± 0.022	0.02128 ± 0.00023	3413 ± 28	0.413	9.30E−06
GJ 699†	M4.0 V	−0.39	3	0.1867 ± 0.0012	This work	3.262 ± 0.022	0.00338 ± 0.00003	3224 ± 10	0.146	3.99E−06
GJ 702A	K0 Ve	0.03	2	0.8310 ± 0.0044	This work	…	0.53 ± 0.02[c] [c]	5407 ± 52	0.846	1.67E−06
GJ 702B	K5 Ve	0.03	2	0.6697 ± 0.0089	This work	…	0.15 ± 0.02[c] [c]	4393 ± 149	0.698	5.90E−06
GJ 725A	M3.0 V	−0.49	3	0.3561 ± 0.0039	This work	3.937 ± 0.004	0.01531 ± 0.00018	3407 ± 15	0.318	5.05E−06
GJ 725B	M3.5 V	−0.36	3	0.3232 ± 0.0061	This work	2.238 ± 0.013	0.00871 ± 0.00012	3104 ± 28	0.235	8.88E−06
GJ 809	M0.5	−0.21	3	0.5472 ± 0.0067	This work	3.224 ± 0.027	0.04990 ± 0.00062	3692 ± 22	0.573	1.41E−05
GJ 880	M1.5 V	0.06	1	0.5477 ± 0.0048	This work	3.502 ± 0.017	0.05112 ± 0.00074	3713 ± 11	0.569	6.66E−06
GJ 892	K3 V	0.07	2	0.7784 ± 0.0053	This work	19.850 ± 0.086	0.26499 ± 0.00152	4699 ± 16	0.763	3.73E−07
GJ 15A†	M1.5V	−0.36	1	0.3790 ± 0.0060	1	5.420 ± 0.044	0.02173 ± 0.00017	3594 ± 30	0.423	2.32E−05
GJ 53A	G5Vp	−0.68	4	0.7910 ± 0.0080	3	25.790 ± 0.147	0.45845 ± 0.00260	5348 ± 26	0.808	3.73E−07
GJ 75	K0V	0.03	2	0.8190 ± 0.0240	3	16.460 ± 0.126	0.51971 ± 0.00396	5398 ± 75	0.837	1.12E−05
GJ 144	K2V	−0.06	2	0.7350 ± 0.0050	5	102.100 ± 0.457	0.32897 ± 0.00147	5077 ± 35	0.781	1.64E−05
GJ 166A†	K1V	−0.24	2	0.7700 ± 0.0210	6	52.690 ± 0.394	0.40782 ± 0.00304	5261 ± 72	0.818	1.03E−05
GJ 380†	K7V	−0.16	2	0.6050 ± 0.0200	4	13.860 ± 0.093	0.10253 ± 0.00069	4203 ± 73	0.669	6.92E−06
GJ 380†	K7V	−0.16	2	0.6490 ± 0.0280	2	13.860 ± 0.093	0.10253 ± 0.00069	4060 ± 87	0.669	6.92E−06
GJ 411†	M2V	−0.41	3	0.3930 ± 0.0080	4	9.842 ± 0.060	0.01989 ± 0.00012	3460 ± 37	0.405	8.04E−06
GJ 411†	M2V	−0.41	3	0.3950 ± 0.0130	2	9.842 ± 0.060	0.01989 ± 0.00012	3457 ± 58	0.405	8.04E−06
GJ 436	M3V	0.04	3	0.4546 ± 0.0182	10	0.788 ± 0.004	0.02525 ± 0.00012	3416 ± 53	0.472	6.84E−06
GJ 551	M5.5V	0.19	5	0.1410 ± 0.0070	6	2.961 ± 0.037	0.00155 ± 0.00002	3054 ± 79	0.118	2.83E−04
GJ 570A	K4V	0.02	2	0.7390 ± 0.0190	6	19.040 ± 0.154	0.20232 ± 0.00163	4507 ± 58	0.743	2.72E−06
GJ 581	M2.5V	−0.10	3	0.2990 ± 0.0100	9	0.930 ± 0.006	0.01130 ± 0.00008	3442 ± 54	0.297	8.28E−06
GJ 699†	M4Ve	−0.39	3	0.1960 ± 0.0080	4	3.262 ± 0.022	0.00338 ± 0.00002	3140 ± 63	0.150	3.99E−06
GJ 764	K0V	−0.19	2	0.7780 ± 0.0080	3	39.670 ± 0.194	0.40926 ± 0.00199	5246 ± 26	0.806	2.61E−06
GJ 820A††	K5V	−0.19	2	0.6650 ± 0.0050	8	37.750 ± 0.188	0.14295 ± 0.00071	4355 ± 17	0.680	5.00E−06
GJ 820A††	K5V	−0.19	2	0.6100 ± 0.0180	2	37.750 ± 0.188	0.14295 ± 0.00071	4548 ± 64	0.680	5.00E−06
GJ 820B††	K7V	−0.29	2	0.5950 ± 0.0080	8	20.340 ± 0.107	0.07753 ± 0.00041	3954 ± 28	0.629	9.28E−06
GJ 820B††	K7V	−0.29	2	0.6280 ± 0.0170	2	20.340 ± 0.107	0.07753 ± 0.00041	3852 ± 53	0.629	9.28E−06
GJ 845	K5V	−0.07	2	0.7320 ± 0.0060	6	50.730 ± 0.505	0.20737 ± 0.00206	4555 ± 24	0.731	1.94E−06
GJ 887††	M0.5V	−0.19	2	0.4910 ± 0.0140	7	10.920 ± 0.127	0.03651 ± 0.00042	3612 ± 53	0.522	5.28E−06
GJ 887††	M0.5V	−0.19	2	0.4590 ± 0.0110	6	10.920 ± 0.127	0.03651 ± 0.00042	3727 ± 47	0.522	5.28E−06

The M-R-L-T_{eff} relations

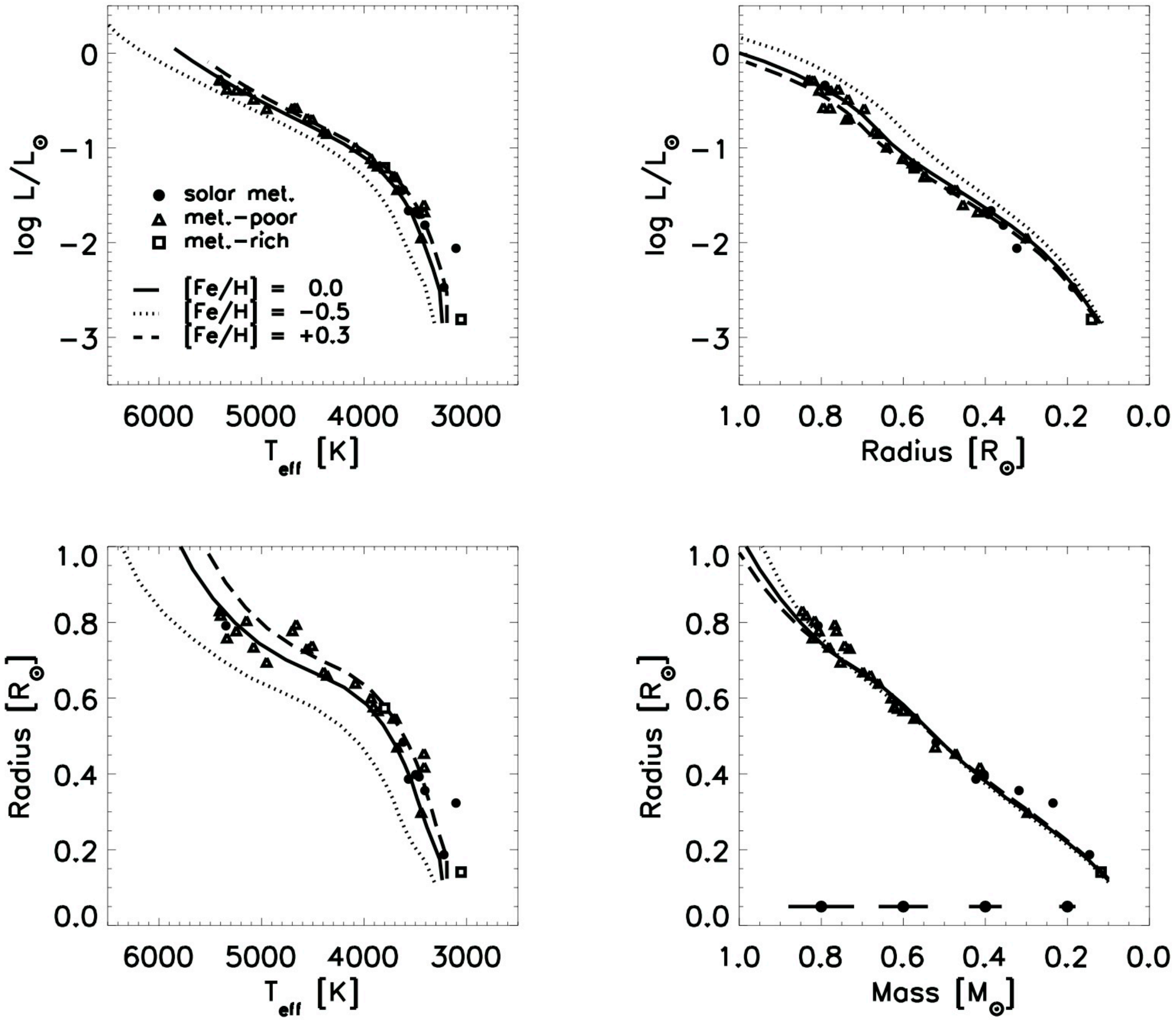

Data: Boyajian et al. (2012)

AIP

The "radius discrepancy"

- Long-standing issue: first reported by, e.g., Hoxie (1973), Lacy (1977)
- Models of solar-like stars (i.e., $M \leq M_{\odot}$) overestimate T_{eff} by ~5% and underestimate R by ~10%
- Luminosity ~constant: surface phenomenon
- Binary vs. single stars
- Disentangle other effects (e.g., age, metallicity)

T_{eff}, R in the single stars sample

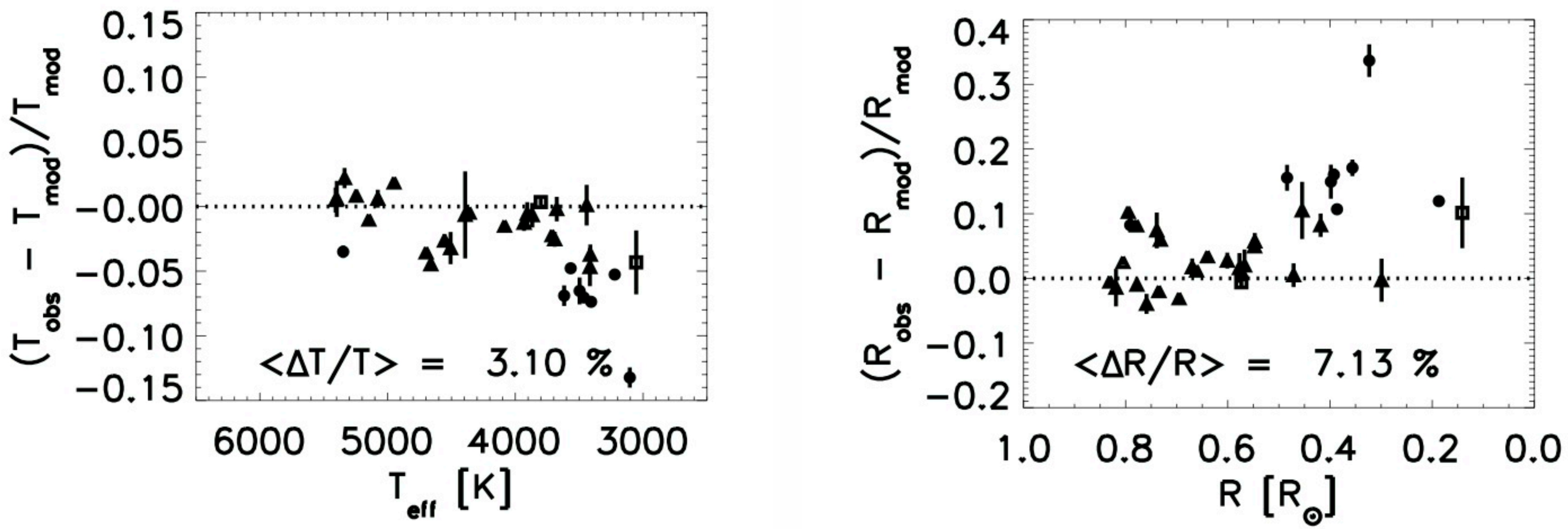

- Literature: $\Delta T_{eff}/T_{eff}$ ~ 5%, $\Delta R/R$ ~ 10%
- Stars with T_{eff} < 4000 K, M < 0.6 $M_\odot$ more affected

Radius discrepancy in single vs. binary stars

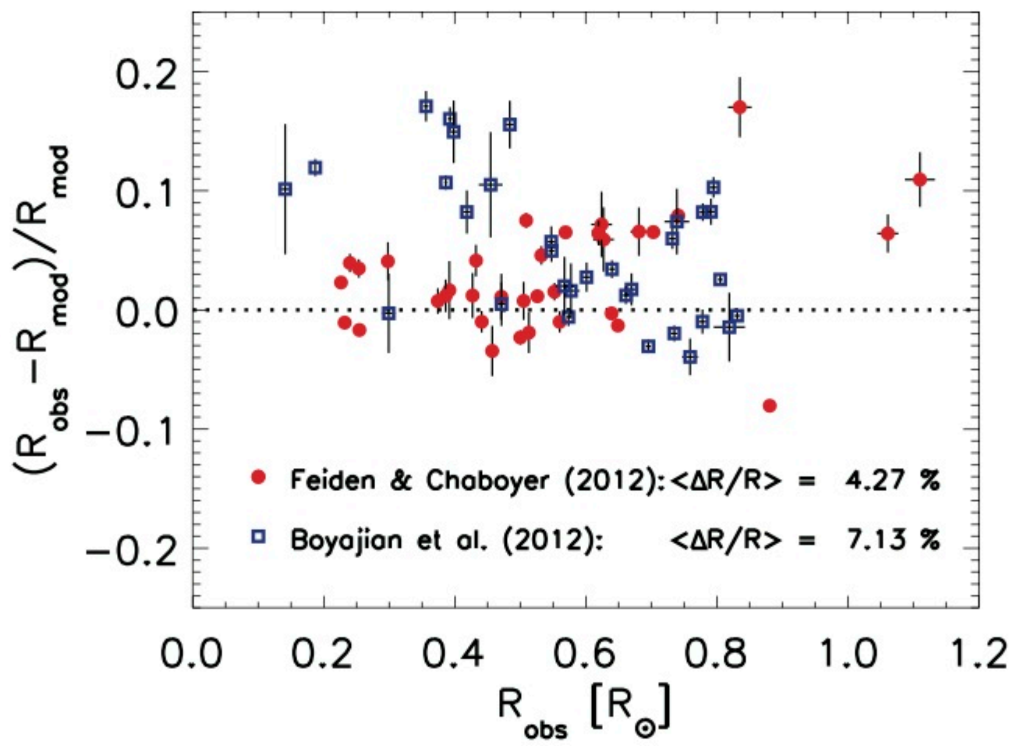

Red: binary stars
Blue: single stars

- Larger discrepancy in the single stars sample
- Discrepancy significant compared to errors for both samples

AIP

Radius discrepancy and activity

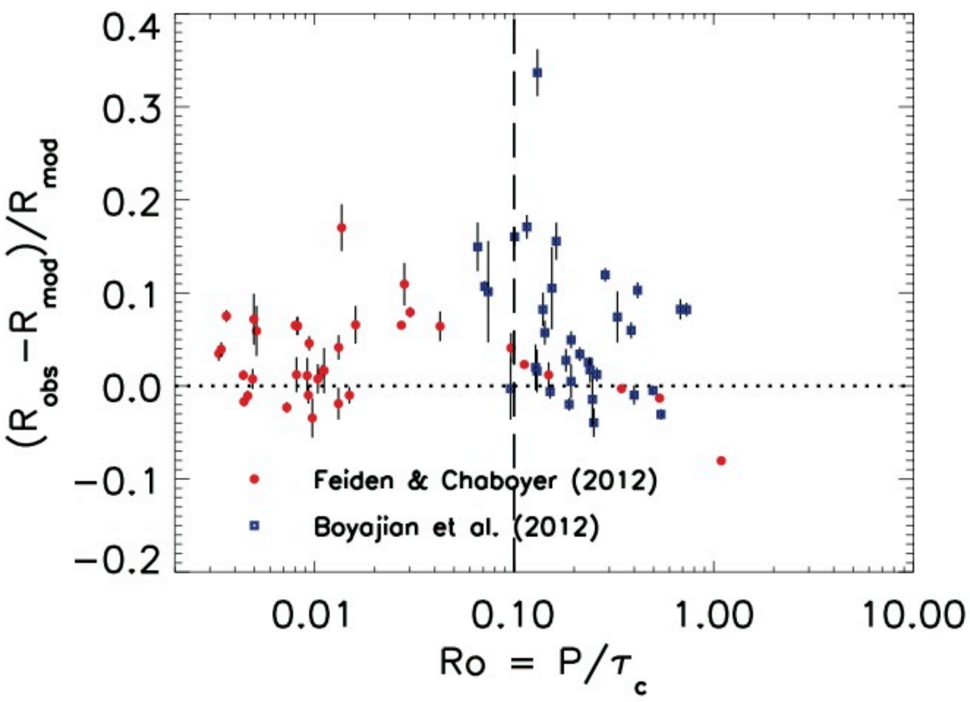

Red: binary stars
Blue: single stars

- Binaries: $P_{rot} \sim P_{orb}$ (tidal synchronization)
- Single stars: P_{rot} obtained from the L_X/L_{bol} – Ro relation (*Wright et al. 2011*)

Surface magnetic fields measurements in low mass stars

- Typical values for measured magnetic fields:
  - G to K stars: 0.01-1. kG
  - M stars: 1-5 kG
- B*f scaling with Ro: age + mass dependence!

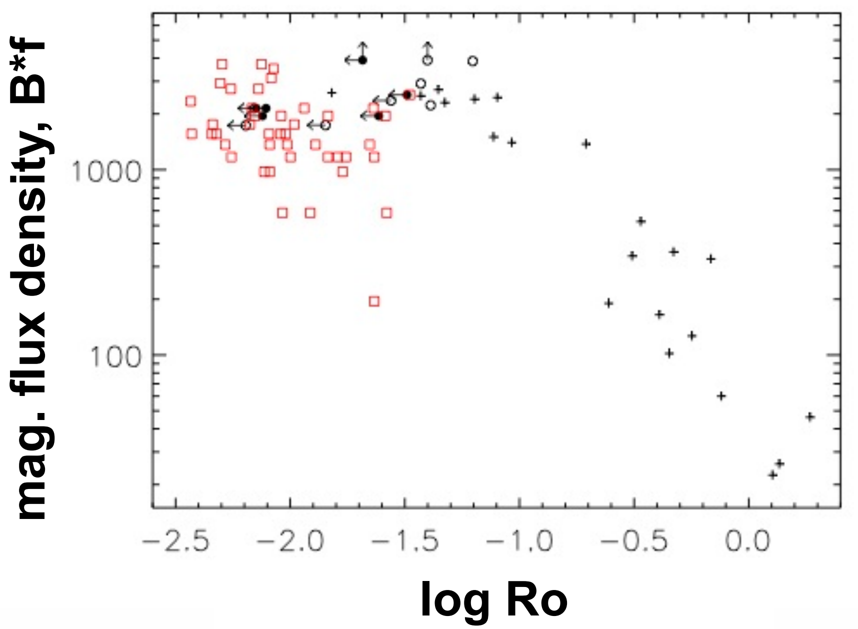

From *Reiners et al. (2009)*

Magnetic activity and stellar models: phenomenological approaches

- Reduced ("effective") MLT parameter α

- Effect of starspots:
  $L = 4\pi R^2 (1-\beta) T_{eff}^4$

- Modified convection criterion:
  (Gough & Tayler, 1966)

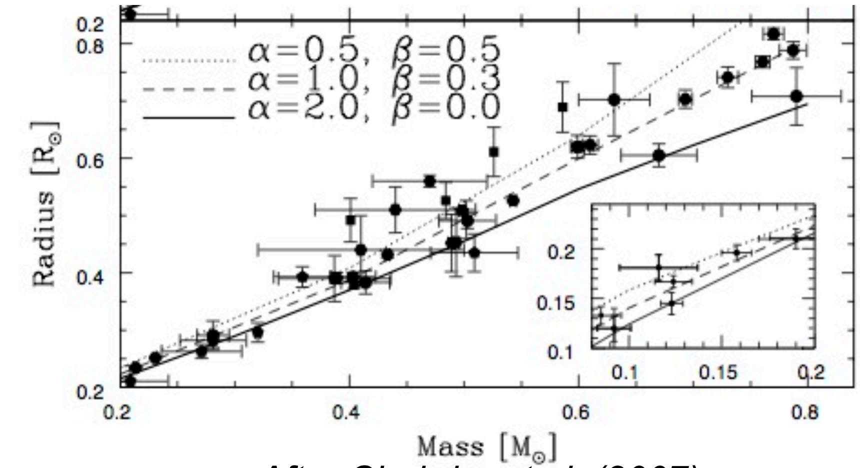

After Chabrier et al. (2007)

$$\nabla_{\rm rad} - \nabla_{\rm ad} > \delta$$

$$\delta = \frac{1}{1 + \gamma \cdot \frac{P_{\rm gas}}{P_{\rm mag}}}$$

Self-consistent approach

Lydon & Sofia (1995): modified thermodynamics, EOS

$$\nabla_{\rm rad} - \nabla_{\rm ad} > -f\frac{\nu}{\alpha}\nabla_{\rm ad}\nabla_\chi - (1-f)\frac{\nu}{\delta}\nabla_\chi$$

$$\chi = \frac{B^2}{8\pi\rho}; \quad \nabla_\chi = \left(\frac{\partial \ln \chi}{\partial \ln P}\right)$$

$$\alpha = \left(\frac{\partial \ln \rho}{\partial \ln P}\right)_{T,\chi}$$

$$\delta = -\left(\frac{\partial \ln \rho}{\partial \ln T}\right)_{P,\chi}$$

$$\nu = -\left(\frac{\partial \ln \rho}{\partial \ln \chi}\right)_{P,T}$$

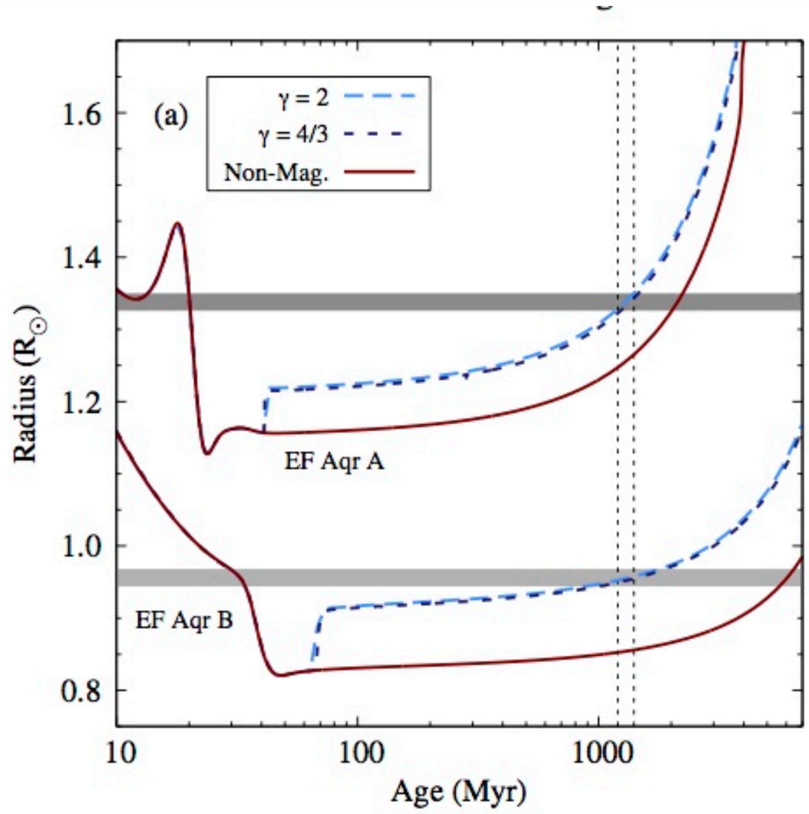

Feiden & Chaboyer (2012)

AIP

Current implementation in YREC

$$\frac{d \log P_\Psi}{d \log M_\Psi} = - f_P \frac{G M_\Psi{}^2}{4\pi r_\Psi{}^4 P_\Psi}$$

$$\frac{d \log T_\Psi}{d \log M_\Psi} = \nabla \frac{d \log P_\Psi}{d \log M_\Psi}$$

$$\frac{d \log r_\Psi}{d \log M_\Psi} = \frac{M_\Psi}{4\pi r_\Psi{}^3 \rho} \text{, and}$$

$$\frac{d L_\Psi}{d \log M_\Psi} = \frac{M_\Psi}{L_o} \ln 10 \left\{ \varepsilon - T_\Psi \frac{dS}{dt} \right\}$$

$$\nabla = \frac{d \ln T}{d \ln P} = \min \left\{ \nabla_{conv}, \frac{f_T}{f_P} \nabla_{rad} \right\}$$

- Magnetic pressure contribution (outer layer, surface B)
- Complete EOS (vs. simple analytical EOS)
- Not self-consistent (yet)!

AIP

Interior structure with magnetic fields

M = 1.0 M⊙

CZ ext. reduced by ~6%

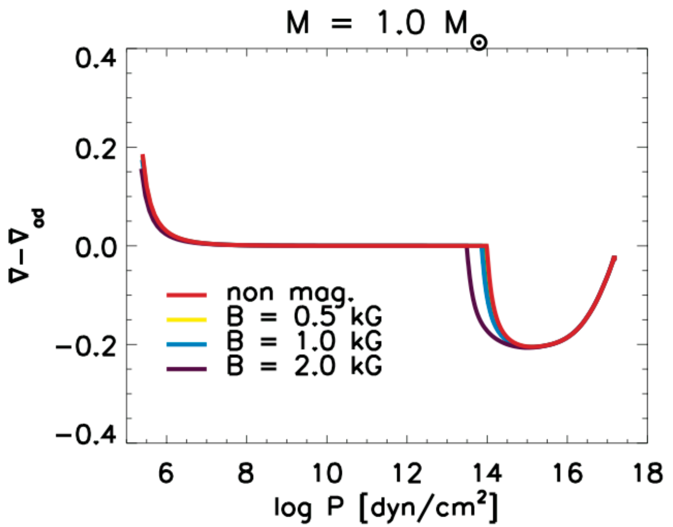

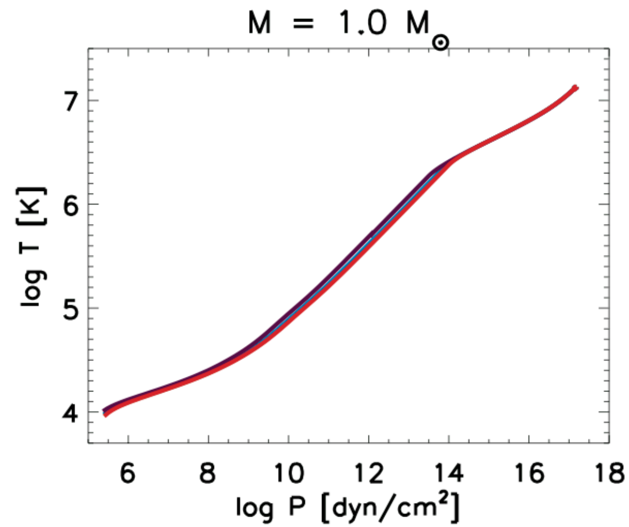

M = 0.6 M⊙

CZ ext. reduced by ~3%

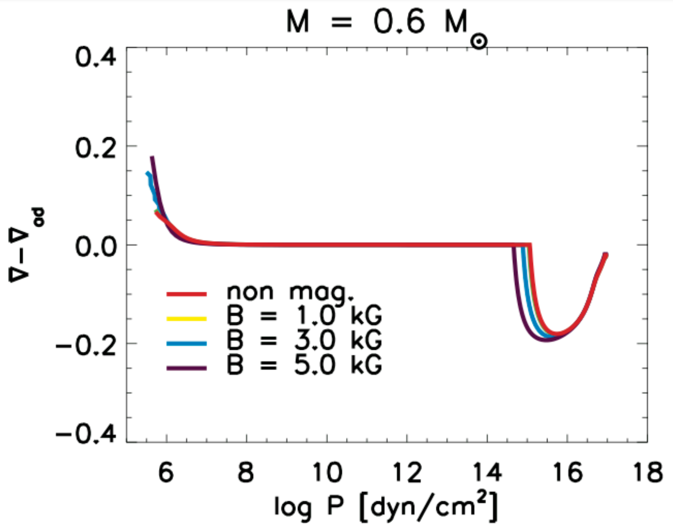

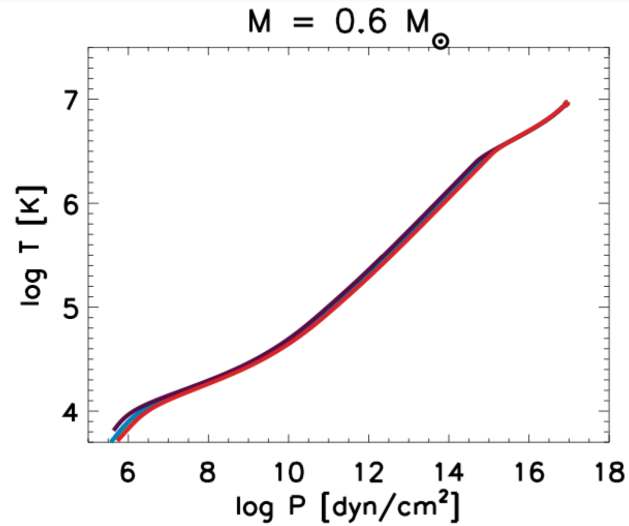

AIP

Evolution of a 1 $M_\odot$ model

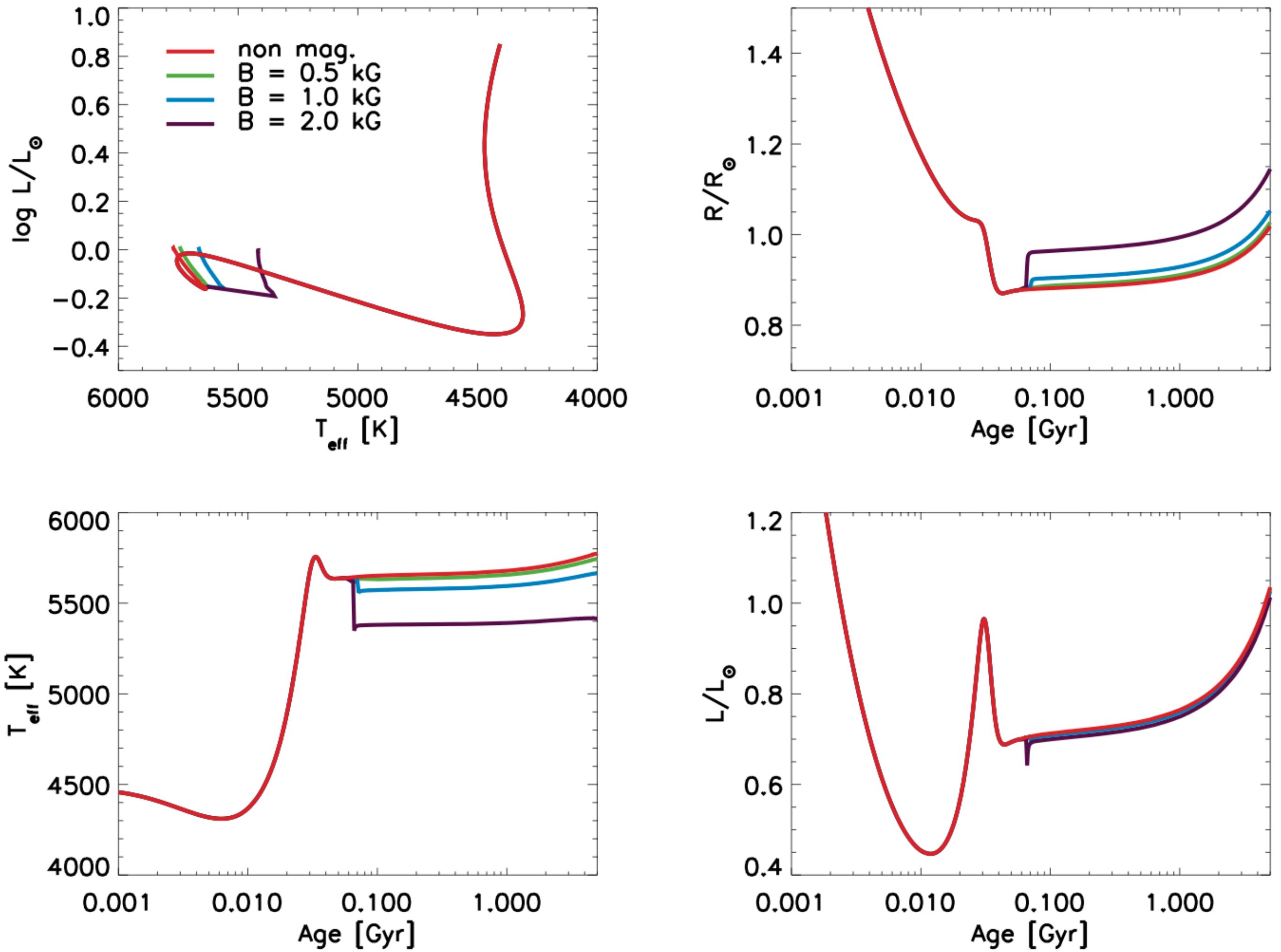

Evolution of a 0.6 $M_\odot$ model

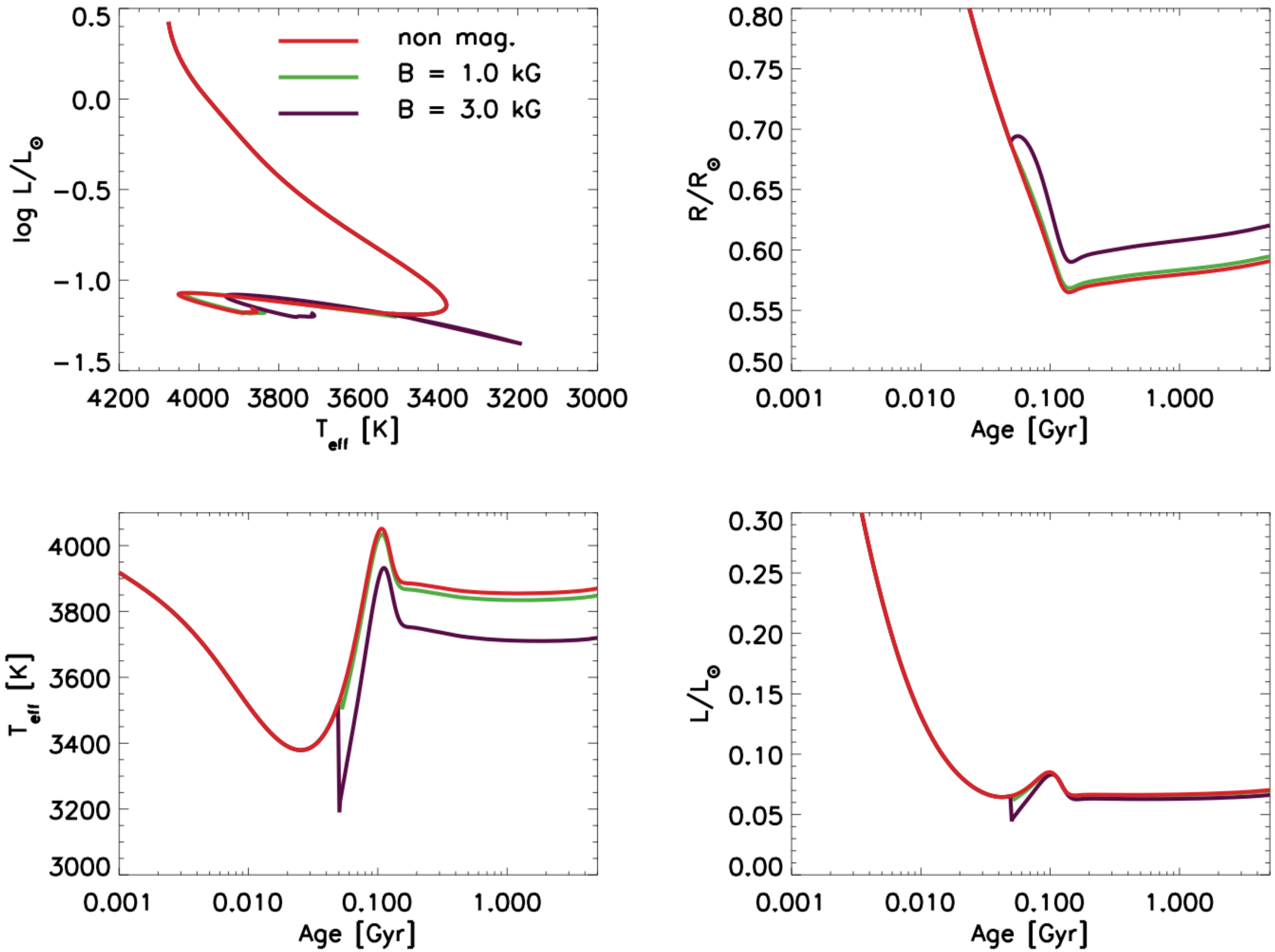

Preliminary results

- Effects of magnetic fields stronger for models of higher mass
- Analogy with sensitivity to the MLT parameter α (efficiency of convection)
- With B = 0.1÷1 kG, ΔR/R comparable to typical “radius discrepancy”

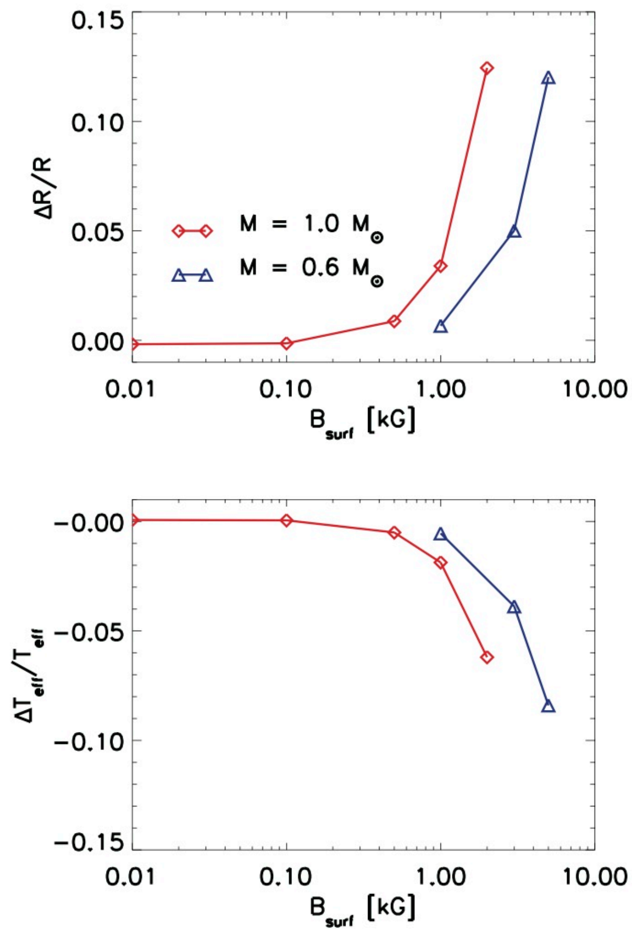

Summary

- The knowledge of fundamental parameters of low mass stars stars is very valuable for many astrophysical applications
- Our models (*Spada et al., in preparation*) improve the Yale-Yonsei isochrones in the $M \leq 0.6\ M_{\odot}$ range and agree satisfactory with observations
- A disagreement between models and observations in R, T_{eff} emerges when using high accuracy measurements in the comparison
- Promising results from models taking into account magnetic fields
- Next step: implement self-consistent treatment of magnetic fields (e.g., Lydon & Sofia 1995); account for radial profile of B